Available online at www.sciencedirect.com
ScienceDirect
Ceramics International 38S (2012) S501–S504
CERAMICS INTERNATIONAL
www.elsevier.com/locate/ceramint

Synthesis of crystalline cerium dioxide hydrosol by a sol–gel method

Hong-Wei He [b], Xiao-Qing Wu [b,*], Wei Ren [b], Peng Shi [b], Xi Yao [b], Zhi-Tang Song [a]

[a] Shanghai Institute of Microsystem and Information Technology, Chinese Academy of Sciences, Shanghai 200050, China
[b] Electronic Materials Research Laboratory, Key Laboratory of the Ministry of Education, Xi'an Jiaotong University, Xi'an 710049, China

Available online 24 May 2011

Abstract

A nano-cerium dioxide hydrosol was synthesized via a sol–gel process at the range of room temperature to 65 °C with the nonionic surfactant PVP (polyvinylpyrrolidone). The mixture solution of cerium nitrate and urea turned out a visible chemical reaction under the catalysis of ammonia. The X-ray diffraction (XRD), transmission electron microscopy (TEM), and X-ray photoelectron spectroscopy (XPS) analyses indicated the colloidal ingredient and nano-crystal structural information. The colloid was crystalline face-centered cubic nano-structured cerium dioxide. The sizes of CeO_2 colloids are in the range of several nanometers to 10 nm or more. The application of the hydrosol may focus on the ceria-based polishing agent for chemical mechanical polishing (CMP) process.

Keywords: A. Sol–gel processes; D. CeO_2; Nonionic surfactant PVP; CMP

1. Introduction

Cerium dioxide is one of the most important rare-earth oxide, of which application fields include industrial catalysts [1,2], solid oxide fuel cells (SOFC) [3,4], polishing abrasive [5,6] and other fields. Especially, CeO_2 polishing abrasive for STI-CMP (Shallow Trench Isolation Chemical Mechanical Polishing) has been received widely attention in recent years due to its excellent selectivity and efficiency. To satisfy polishing requirements, a variety of cerium oxide synthesis methods have been extensively studied to increase cerium dioxide performance in STI-CMP process, such as precipitation, sol–gel, hydrothermal, physical chemistry, and high-energy dispersion.

As we known, the commercial abrasive particles are usually prepared by means of calcination, gas combustion or high-energy ball milling dispersion, easily leading to irregular shape, severe agglomeration, uneven distribution of particles. These disadvantages resulted in the scratches and defects of polished surface, and limited the CeO_2 abrasive further application in the decreasing feature size of integrated circuits in the semiconductor industry.

In this paper, we proposed to replace CeO_2-calcinated abrasive with CeO_2-colloid abrasive in order to reduce polishing defects. Otherwise, the synthesized colloids should be crystalline ceria to keep its high polishing selectivity.

2. Experimental

The synthesis process was similar to the reference [7,8]. The details were described as follows (Fig. 1): cerium source $Ce(NO_3)_3{\cdot}6H_2O$, buffer $CO(NH_2)_2$ and dispersant PVP were dissolved into a certain amount of deionized water with a magnetic stirrer. The temperature of the mixture solution gradually increased from room temperature to the set temperature, and the solution should be kept stirring for 1 h. Then, an appropriate amount of ammonia was added dropwise with a burette. The reaction quickly happened within a few seconds, and the solution color underwent obviously change in few hours. The phenomenon of color change was believed to be correlated with the chemical changes. As the color of reaction solution turned from purple into pale yellow, the Ce^{3+} happened to be oxidized into Ce^{4+} by O_2 under air atmosphere. The possible chemical reaction is stated as the following formulas [9]:

$$Ce(NO_3)_3{\cdot}6H_2O + 3NH_3{\cdot}H_2O \rightarrow Ce(OH)_3\downarrow + 3NH_4NO_3 + 6H_2O \quad (1)$$

* Corresponding author. Tel.: +86 29 82668679; fax: +86 29 82668794.
E-mail address: xqwu@mail.xjtu.edu.cn (X.-Q. Wu).

0272-8842/$36.00
doi:10.1016/j.ceramint.2011.05.063

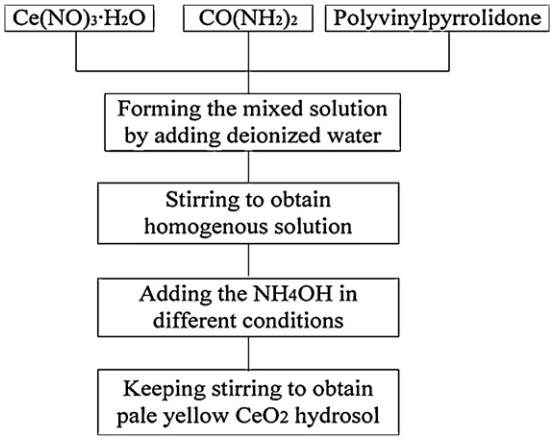

Fig. 1. Flow chart for synthesis process of cerium dioxide.

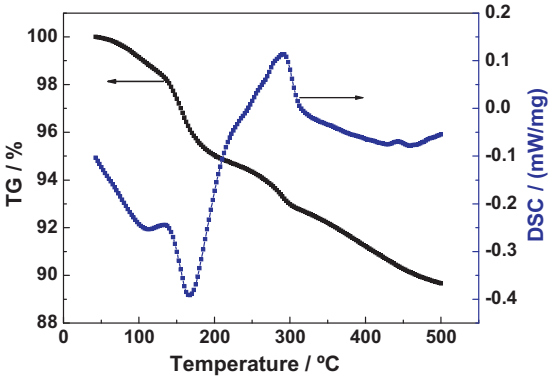

Fig. 2. TG–DSC curves of the dried ceria powder.

$$4Ce(OH)_3 + O_2 + 2H_2O \rightarrow 4Ce(OH)_4 \downarrow \quad (2)$$

$$Ce(OH)_4 \cdot nH_2O \rightarrow CeO_2 \cdot xH_2O + yH_2O \quad (x + y = n) \quad (3)$$

In the step of Eq. (1), the solution color is purple. Then, the color turns from purple into white and pale yellow orderly, corresponding to Eqs. (2) and (3), respectively.The equipment NETZSCH STA 449 was used to carry out a thermal analysis. The structure information of colloid was confirmed by Rigaku D/MAX2400 X-ray diffractometer. X-ray photoelectron spectroscopy was measured by ESCALAB VG-MK-II to confirm the oxidation state of the cerium. JEM-3010 transmission electron microscopy (TEM) was adopted to characterize the shape, size and crystal structure of ceria colloids.

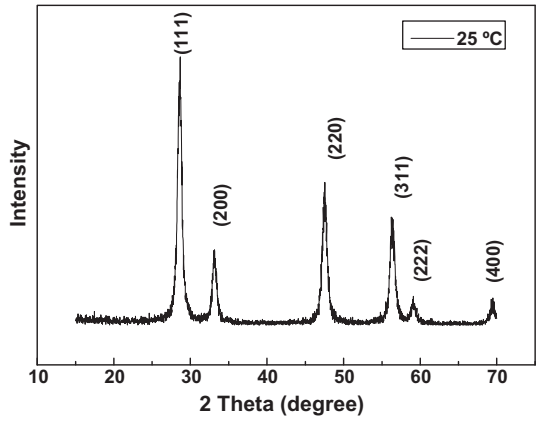

Fig. 3. X-ray diffraction pattern of the dried ceria colloids.

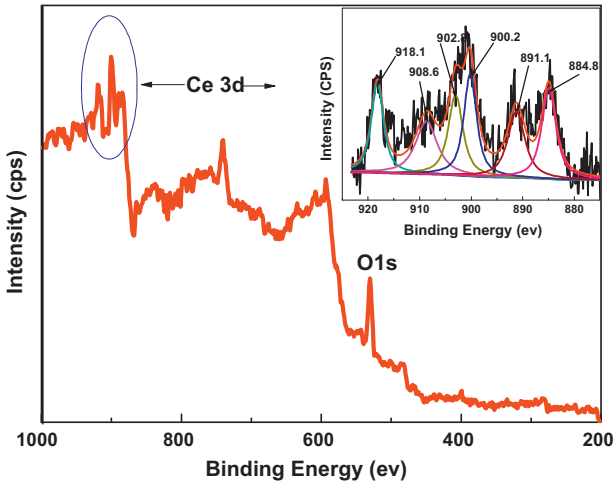

Fig. 4. XPS spectrum and Ce 3d XPS spectrum (inset) of the sample.

3. Results and discussion

In order to confirm the possible compound in the powder sample for researching the actual reaction process, the sample was dried at room temperature in the semi-closed crucible for several days. The dried powder showed pale yellow, as the same color as the sol. Fig. 2 shows the TG–DSC curves of the dried powder.

The TG–DSC patterns (in Fig. 2) showed the thermal behavior from room temperature up to 500 °C. The mass loss can be divided into four stages: The weight loss below 140 °C

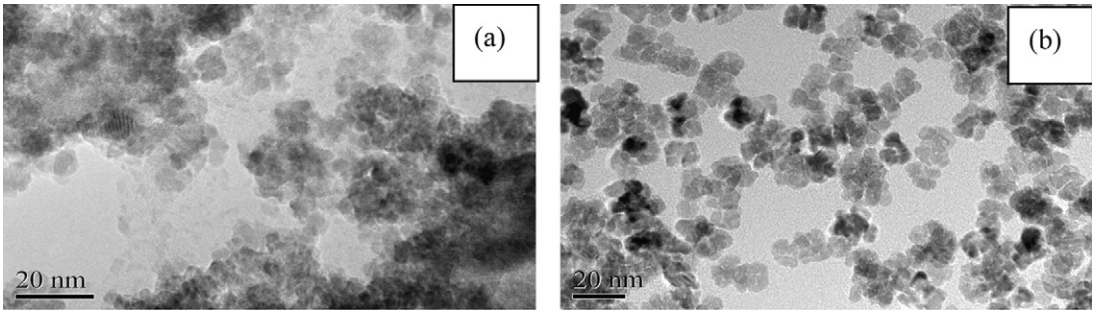

Fig. 5. (a) TEM image of CeO_2 prepared at 25 °C; (b) TEM image of CeO_2 prepared at 65 °C.

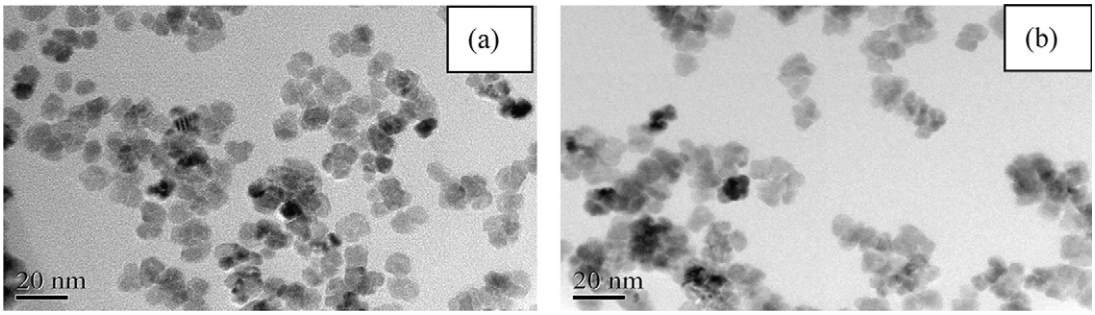

Fig. 6. TEM images of CeO_2 prepared CeO_2 with different cerium concentrations: (a) 0.05 mol L^{-1}; (b) 0.1 mol L^{-1}.

was due to the removal of physisorbed water. Decomposition of the structural water was in between 140 °C and 215 °C. The weight loss from 215 °C to 305 °C was attributed to the decomposition of a side product of cerium oxycarbonate [7], corresponding to a sharp exothermic peak at 291 °C in the DTA curve. The exothermic peak around 450 °C might be caused by the oxidation of cerium compound. So, it could be concluded that the synthesized product contained not only ceria but also some other materials.

As we know, the crystal structure of pure ceria is a face-centered cubic structure, grouped into the calcium fluoride (CaF_2) structural type with space group Fm3m. The XRD pattern of the dried ceria colloids (Fig. 3) showed a good agreement with literature data (JCPDS No. 34-0394). The main Bragg peaks with Miller indices (1 1 1), (2 0 0), (2 2 0), (3 1 1), (2 2 2), and (4 0 0) could be found clearly. The pure crystallized ceria could be obtained at lower temperature.

Fig. 4 depicts the XPS spectrum of the CeO_2 nanoparticles. Peaks of Ce 3d and O 1s proved the existence of cerium oxide. Ce 3d binding energy (BE) peaks were consistent with that of Ce^{4+} ions. The band at 918.1 eV should be one of the $3d^{10}4f^0$ state of the Ce^{4+} ions [10,11], compared with the band of 916.5 eV BE in the reference [12], the upward shift of binding energy value may be due to smaller particle size. Here, the software of XPSPEAK41 was used to mark and fit the Ce 3d peaks.The aqueous solution with concentration of 0.1 mol L^{-1} cerium was adopted for synthesis of ceria colloids. The content of PVP was 30 g L^{-1}. The TEM images of ceria colloids synthesized at different temperatures for 72 h are shown in Fig. 5. Obviously, the sample synthesized at 25 °C had severe colloid agglomeration (Fig. 5(a)). However, the sample synthesized at 65 °C (Fig. 5(b)) indicated a better dispersing behavior. Lower temperature might restrain the dispersion effect of PVP so that leaded to a bad dispersion performance. It means that the dispersion effect of PVP requires a proper temperature.

Generally, the content of ceria colloids in the solution depends on the concentration of cerium salt in reaction precursor. In the study, the samples with different cerium contents were synthesized to confirm the limit concentration of ceria hydrosol. The experimental results shown: with increasing concentration of cerium salt in the solution, the precipitation started to appear gradually. When the concentration of cerium reached up to 0.2 mol L^{-1}, the colloids in the solution could not keep its suspension state and formed precipitation totally. Fig. 6 shows the TEM images of two kinds of cerium concentration samples. It could be found that each colloid was consisted of several 10-nm-size crystal particles, and ceria colloids were not monodispersed actually. The CeO_2 colloids obtained from the solution of 0.05 mol L^{-1} cerium (a) possessed a better dispersion performance than that of

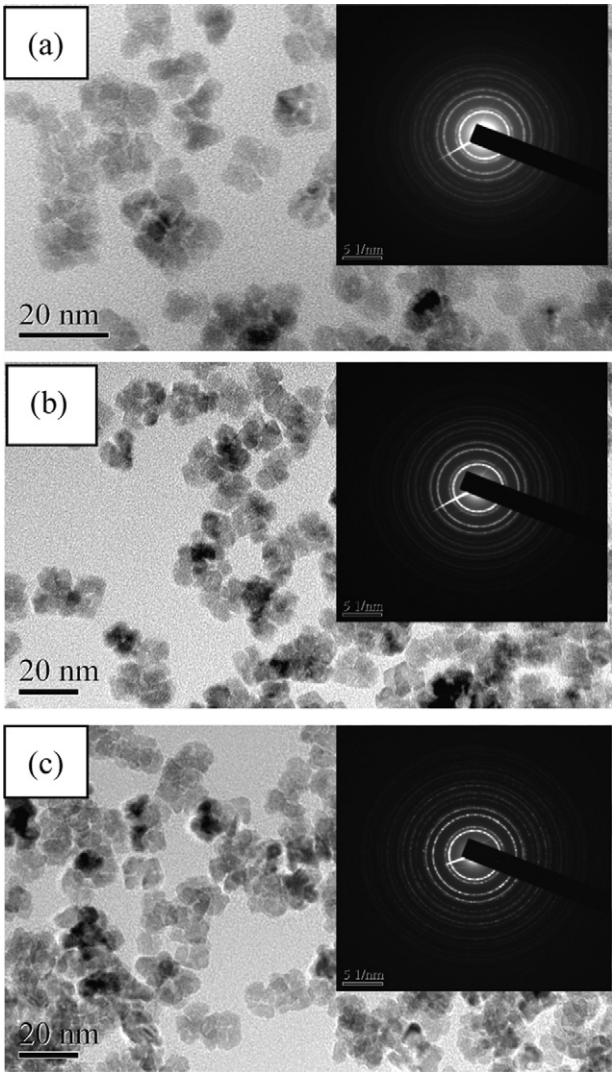

Fig. 7. TEM images of CeO_2 prepared at 65 °C with different times: (a) 8 h, (b) 24 h, and (c) 72 h.

0.1 mol L^{-1} cerium (b). The experimental facts indicated the stability of ceria hydrosol is relative to the concentration of cerium salt.

Fig. 7(a)–(c) shows TEM images of the samples prepared at different reaction times. It could be seen that the effect of reaction time on crystallinity of ceria is obvious. With increase of reaction time, the reciprocal lattice of patterns became more and more evident, which proved a well-crystallized ceria. Size of the ceria colloids not changed obviously with increase of reaction time.

Ceria particles are easy to form aggregation. To verify the stability of cerium oxide hydrosol, the sample stored three months was measured by TEM. The colloids had no significant further agglomeration compared with fresh sample (similar to Fig. 7). The hydrosol is stable enough for application.

4. Conclusions

Well-dispersed ceria hydrosol was obtained via the sol–gel process at 65 °C. The ceria colloids possessed face-centered cubic CaF_2 structure. The grain size is in the range of several nanometers to more than 10 nm. The hydrosol also exhibited a good aging stability in three months.

References

[1] S. Salomons, R.E. Hayes, M. Votsmeier, A. Drochner, H. Vogel, S. Malmberg, J. Gieshoff, On the use of mechanistic CO oxidation models with a platinum monolith catalyst, Applied Catalysis B: Environmental 70 (2007) 305–313.

[2] C. Agrafiotis, A. Tsetsekou, C.J. Stournaras, A. Julbe, L. Dalmazio, C. Guizard, Evaluation of sol–gel methods for the synthesis of doped-ceria environmental catalysis systems: Part I. Preparation of coatings, Journal of the European Ceramic Society 22 (2002) 15–25.

[3] B. Ksapabutr, E. Gulari, S. Wongkasemjit, Sol–gel derived porous ceria powders using cerium glycolate complex as precursor, Materials Chemistry and Physics 99 (2006) 318–324.

[4] V.V. Kharton, A.A. Yaremchenko, A.A. Valente, E.V. Frolova, M.I. Ivanovskaya, J.R. Frade, F.M.B. Marques, J. Rocha, Methane oxidation over SOFC anodes with nanocrystalline ceria-based phases, Solid State Ionics 177 (2006) 2179–2183.

[5] R. Sabia, H.J. Stevens, J.R. Varner, Pitting of a glass-ceramic during polishing with cerium oxide, Journal of Non-Crystalline Solids 249 (1999) 123–130.

[6] X.D. Feng, D.C. Sayle, Z.L. Wang, M.S. Paras, B. Santora, A.C. Sutorik, T.X.T. Sayle, Y. Yang, Y. Ding, X.D. Wang, Y.S. Her, Converting ceria polyhedral nanoparticles into single-crystal nanospheres, Science 312 (2006) 1504–1508.

[7] B. Bakiz, F. Guinneton, J.P. Dallas, S. Villain, J.-R. Gavarri, From cerium oxycarbonate to nanostructured ceria: relations between synthesis, thermal process and morphologies, Journal of Crystal Growth 310 (2008) 3055–3061.

[8] Q. Li, Z.H. Han, M.W. Shao, X.M. Liu, Y.T. Qian, Preparation of cerium hydroxycarbonate by a surfactant-assisted route, Journal of Physics and Chemistry of Solids 64 (2003) 295–297.

[9] X.D. Zhou, W. Huebner, H.U. Anderson, Room-temperature homogeneous nucleation synthesis and thermal stability of nanometer single crystal CeO_2, Journal of Applied Physics Letters 80 (2002) 3814–3816.

[10] T.D. Nguyen, T.O. Do, General two-phase routes to synthesize colloidal metal oxide nanocrystals: simple synthesis and ordered self-assembly structures, Journal of Physical Chemistry C 113 (2009) 11204–11214.

[11] H.X. Mai, L.D. Sun, Y.W. Zhang, R. Si, W. Feng, H.P. Zhang, H.C. Liu, C.H. Yan, Shape-selective synthesis and oxygen storage behavior of ceria nanopolyhedra, nanorods, and nanocubes, Journal of Physical Chemistry B 109 (2005) 24380–24385.

[12] F. Kapteijn, A.D. Langeveld, J.A. Moulijn, A. Andreini, M.A. Vuurman, A.M. Turek, J.M. Jehng, I.E. Wachs, Alumina-supported manganese oxide catalysts: I. Characterization: effect of precursor and loading, Journal of Catalysis 150 (1994) 94–104.